Self-Similarity and Pattern Selection in the Roughening of Binary Liquid Films

Harald Hoppe, Marcus Heuberger, and Jacob Klein*
Weizmann Institute of Science, Rehovot 76100, Israel
(Received 5 January 2001)

Films of spinodally decomposing binary liquid mixtures show transient wetting of both confining interfaces by one of the phases, and rupture, with characteristic wavelength λ_c and time τ_{rupture}, leading to flat droplets of the nonwetting phase encapsulated by the wetting phase. Over the entire range of film thicknesses $d \approx 100-3500$ nm, we find $\tau_{\text{rupture}} \propto d^{1.01\pm0.08}$, indicating film structures that scale self-similarly with d, and find also that $\lambda_c \approx 60 d^{0.97\pm0.03}$, the large prefactor suggesting a rupture wavelength which minimizes the interfacial tension of the roughened film.

DOI: 10.1103/PhysRevLett.86.4863 PACS numbers: 68.15.+e, 47.20.Dr, 68.55.–a

The stability and breakup of thin liquid films on solid substrates is a subject of considerable practical and fundamental interest. While the behavior of single component films has been extensively studied and is by now reasonably well-understood [1–4], the behavior of liquid mixtures presents a great richness of behavior, primarily due to the complex interplay between wetting and spinodal demixing [5–10]. The case of immiscible binary (A/B) liquid mixtures in thin films, where one of the coexisting phases wets both confining interfaces, has received particular attention in recent years [6,10–13]. The picture that has emerged is as follows: When a film of such a fluid at critical or near critical composition is taken into the two-phase regime, it initially undergoes simultaneous spinodal decomposition and an initial transient wetting of both confining surfaces by the wetting phase. As the wetting layers at the external interfaces thin, the region between them (consisting of a bicontinuous network of the two coexisting phases) coarsens. For the case where one of the interfaces is air or vacuum, this internal coarsening leads to roughening of the film at that surface [7], and the eventual formation of droplets of the nonwetting phase encapsulated by the wetting one [6]. Different mechanisms for the breakup and structure of such films have been adduced, ranging from anomalous surface roughening induced by the phase separation [6] to so-called spinodal dewetting induced by capillary fluctuations [13]. Here, we examine systematically the breakup of such binary fluid films as a function of their thickness. Our results reveal a strongly linear relationship, over some one-and-a-half decades, both between the rupture time τ_{rupture} of the films and their thickness d, and between the characteristic surface rupture wavelength λ_c and d. They show that $\lambda_c = \text{const} \times d$, where the magnitude of the constant prefactor is comparable to (γ_A/γ_{AB}), γ_A being the surface tension of the wetting phase and γ_{AB} the A/B interfacial tension. This suggests, intriguingly, that the characteristic initial surface rupture dimension is selected so as to minimize the overall interfacial energy of the emerging droplet-decorated film.

The binary fluid mixtures consist of two statistical copolymers (kindly donated by Dr. L. J. Fetters), each of structure $\{[C_4H_8]_{(1-x)}\text{-}[C_2H_3\text{—}(C_2H_5)]_x\}_N$, with different x values, where the diethyl ($[C_4H_8]$) and the ethylethylene $\{[C_2H_3\text{—}(C_2H_5)]\}$ monomers are distributed randomly on the chains. N are the degrees of polymerization of the copolymers. Within each pair, one of the components is partially deuterated (and labeled dx_j, with x in %; the other—fully hydrogenated—component is labeled hx_i) to enable composition depth profiling by nuclear reaction analysis [14,15] (NRA). Mixtures of $h78$ and $d95$, and of $d78$ and $h95$, were studied, their degrees of polymerization being $N_{78} = 1290$ and $N_{95} = 2507$, respectively. The interaction between such molecules depends in a known manner [16] on the mean branching ratio $\frac{1}{2}(x_i + x_j)$ and on the difference $|x_i - x_j|$. Thin films of symmetric composition (50:50 wt %, near the critical composition $\phi_{c,d95} = 42$ wt %) were spin cast from toluene solutions onto polished silicon wafers (ca. 1 cm × 1 cm), cleaned prior to coating by sonication in toluene. The film thickness, controlled by solution concentration and spin frequency, was varied between 100 nm up to more than 3 μm and checked by ellipsometry. Each sample was then placed on a heating plate in a small vacuum chamber, and monitored through a window by a reflecting optical light microscope. Once vacuum was established, the samples were heated from room temperature to 150 °C within seconds. A CCD camera was used for subsequent digitalizing, and the pictures were stored on a coupled PC. To investigate the three-dimensional topography of the final structures on the film, optical phase interference microscopy (OPIM) was used. NRA was applied to study the composition vs depth variation within the films at different times.

Typical development of the films with time is shown in Fig. 1 for a film of thickness 970 ± 30 nm. Immediately after spin coating, the films appeared smooth and laterally homogeneous. On annealing (for a time dependent on the film thickness), the surface started to roughen, as shown in Fig. 1(a). At longer times, Fig. 1(b), cracks or ruptures over the entire sample appeared at about the same time τ_{rupture}, with a characteristic spacing λ_c between them. Between the rupture sites, the surface shows

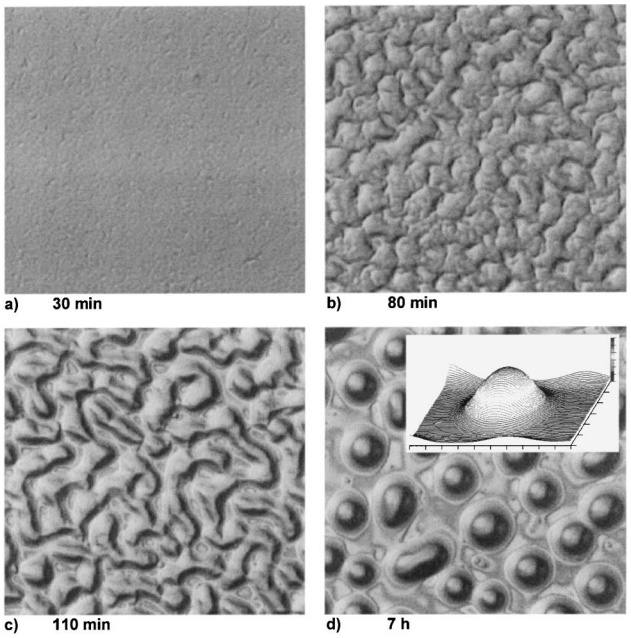

FIG. 1. Development with time of the spin-cast, initially smooth film of the $d95/h78$ liquid mixture at 150 °C recorded with a CCD camera (initial film thickness 970 ± 30 nm). The film roughness increases with time: It is slightly rough in (a) 30 min, much rougher at (b) 80 min, and the film eventually ruptures at a characteristic spacing λ_c. The resulting wormlike structure is subsequently smoothed (c), and finally forms droplets (d), which grow by slow coalescence. The pictures show a section of about 0.7 mm × 0.7 mm while the scale bars in the inset of (d) have a dimensions of 192 μm × 144 μm × 3.8 μm (height).

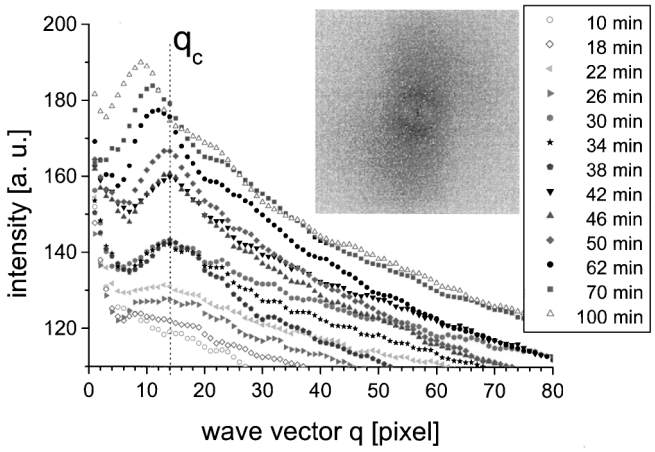

FIG. 2. Development with time of the power spectrum of the circular averaged 2D FFT (e.g., inset) for a film of 888 ± 15 nm thickness. Over a period of some 20 min ($t = \sim 30-50$ min), the position of the peak—corresponding to the characteristic spacing λ_c—remained at a constant position q_c. For $t > \sim 50$ min, the peak shifts to smaller wave vectors q, corresponding to film coarsening [(as in Figs. 1(c) and 1(d)]. (Here the wavelength relates to q as $\lambda = 656.4/q$ μm, where q is in pixels.)

a transient roughness on a smaller scale, which disappears as the film breaks up into round or worm-shaped droplets [Fig. 1(c)]. These smoothed wormlike structures may undergo Rayleigh instabilities and at long times contract into flat bell-shaped droplets [Fig. 1(d)]. The droplets were imaged by OPIM, which revealed their three-dimensional structure as visible in the inset of Fig. 1(d). The valleys between the droplets never reach the silicon surface, as it remains covered at all times by a stable wetting film. Finally [as indicated in the lower left of center in 1(d)], the droplets slowly coalesce into ever-larger drops.

A sequence of pictures for a number of samples were analyzed by a two-dimensional (2D) fast Fourier transform (FFT) over a square section of 512 × 512 pixels, and these were radially averaged to provide a 1D power spectrum. An example is shown in Fig. 2. Initially, the spectrum has no marked features, but after a time a characteristic wave vector is indicated by a small bump in the power spectrum, at $q \approx 14$ pixels. The amplitude of this peak increases, and over a significant period—from ca. 30 min up to ca. 50 min for the sample of Fig. 2—its wave vector, labeled "q_c" in Fig. 2, remains constant. At longer times, the peak position slowly shifts towards smaller wave vectors, as a result of the formation of the droplets and their further growth by coalescence. The central result of this FFT analysis of the film coarsening is the identification of a single marked wavelength λ_c, which can be confidently determined within a certain time window, characteristic of those growing indentations which lead to rupture.

Such characteristic wavelengths λ_c were determined as above as a function of film thickness d. In addition, from the time sequence of the film structure evolution, we were able to estimate the time τ_{rupture} at which the largest undulations ruptured the film surface and holes or cracks first appeared. These variations are plotted in Fig. 3. Over the range of parameters in our study, covering a variation of some 35-fold in d, the data show a strongly linear variation, with $\lambda_c \propto d^{0.97\pm0.03}$ and $\tau_{\text{rupture}} \propto d^{1.01\pm0.08}$.

The early time development of the phases perpendicular to the sample surface was studied via NRA composition-depth profiling. Thin films ($d \approx 1$ μm) of both the $h78/d95$ mixture and the complementary pair $d78/h95$ were prepared, enabling both phases to be profiled independently. Annealing times were chosen to be sufficiently short so that the profiles would still be unperturbed by the roughening (which starts after several minutes). In Fig. 4(a), the symmetric wetting of the $d95$-rich phase at both external interfaces is shown for an annealing time of only 40 ± 10 s. Some time later [250 ± 10 s, Fig. 4(b)] the wetting layers are substantially depleted; hence, a backflow of the $d95$-rich phase from the surfaces into the central part of the film must have taken place. We note that the transient wetting layer develops sufficiently fast at the temperature of our measurements that we could not observe the early and intermediate stages by which it was built up, as the annealing times required are too short to be accessible to us. Note that the composition profile of

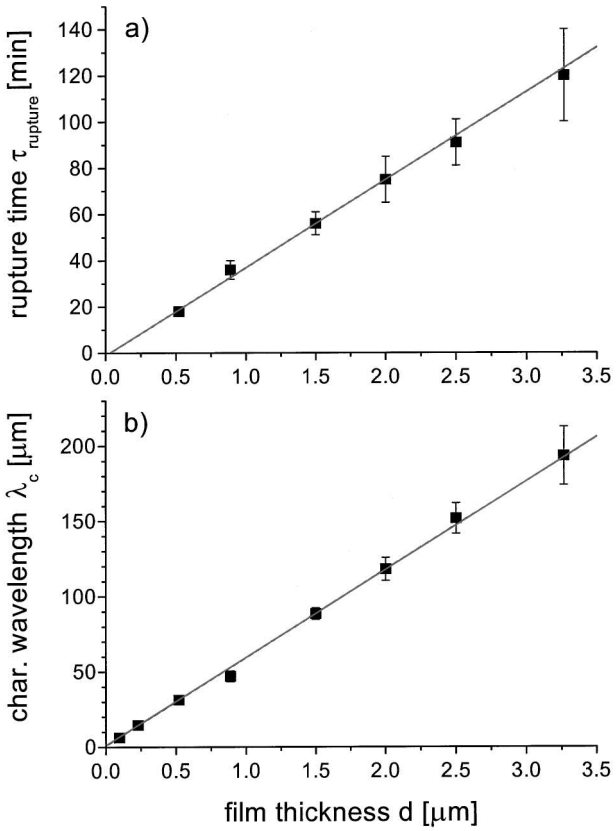

FIG. 3. Dependence on the film thickness d of (a) the rupture time τ_{rupture} and (b) the characteristic wavelength λ_c. Error bars in (a) are due to uncertainties in τ_{rupture} of the order of the time between up to three consecutive images (or up to five consecutive images for the thickest films); those in (b) for λ_c are due to uncertainties of the order of a pixel in q_c.

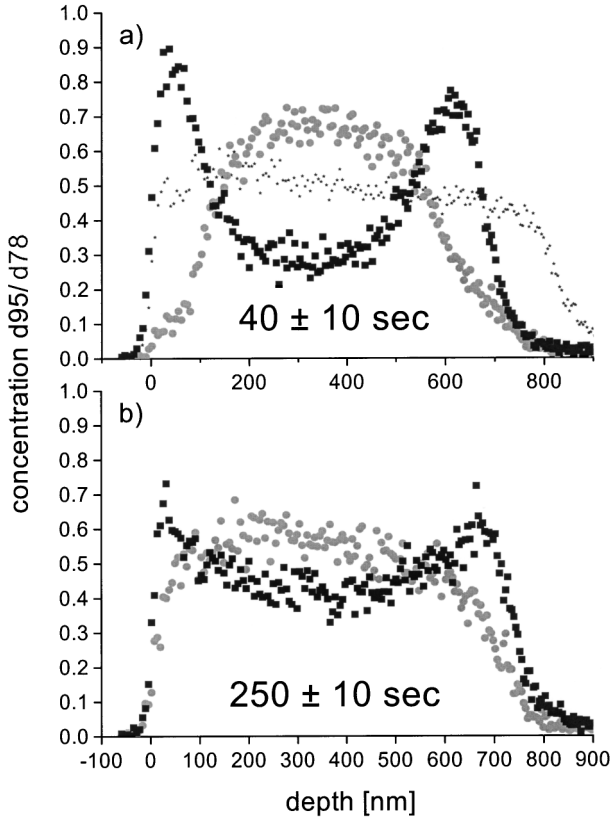

FIG. 4. NRA composition-depth profiles of spin cast $d95/h78$ and $h95/d78$ films at short annealing times t at 150 °C. Profiles in all cases are of the deuterated component [$d95$ (■); $d78$ (solid grey circles)]. (a) $t = 40 \pm 10$ s. The $d95/h78$ mixture (■) shows clear peaks at the film interfaces corresponding to wetting layers of the $d95$-rich phase, while the complementary $h95/d78$ profile (solid grey circles) mirrors this in showing depletion of the $d78$-rich phase at the film interfaces. The composition profiles (★) in the as-cast $d95/h78$ film ($t = 0$) are flat and uniform, showing that the wetting revealed in (a) has taken place over 40 s or less. (b) $t = 250 \pm 10$ s. The peaks corresponding to the wetting layers of the $d95$-rich component (■) are greatly reduced, mirrored by the smaller depletion of $d78$ (solid grey circles) at these interfaces.

an as-cast film prior to annealing—stars in Fig. 4(a)—is essentially uniform, with no evidence for excess of the wetting component ($d95$) at either surface. We conclude therefore that the wetting layers (in the films shown in Fig. 4) build up rapidly ($t < 1$ min) but are then depleted more slowly (of the order of several minutes).

What do the linear d dependences of both λ_c and τ_{rupture} tell us about the roughening mechanism? Earlier work by Bodensohn and Goldburg [11] and by Tanaka [10] investigated confined binary fluid mixtures, where, as in our system, one of the coexisting phases wets both walls: They find that the wetting layers build up rapidly from the spinodally demixed phases within the film, via flow of the wetting phase to the surfaces. Such flow is driven hydrodynamically and, as recently demonstrated [17], the resulting surface wetting layers thickness l_w grows linearly with time, $l_w \propto t$. These surface layers are connected via channels of the wetting phase to the bicontinuous two-phase network in the bulk of the film. Coarsening of the network with t also takes place, and channels, of radius $a(t)$, grow in the so-called viscous hydrodynamic regime [18,19], at a rate $(da/dt) \propto (\gamma_{AB}/\eta)$, where η is the viscosity of the wetting phase. As described by Tanaka, however [10], once $a \gtrsim d/2$, the Laplace pressure within the channel becomes smaller than within the wetting layers, and the hydrodynamically driven flow into the wetting layer is reversed. The wetting phase is then "pumped" back into the central biphasic region of the film, depleting the wetting layers [10]. Such a depletion of the wetting layers after their initial rapid buildup is indeed observed in our study (Fig. 4).

Our results may now be readily understood. As annealing commences, the wetting layers l_w start to grow, while at the same time coarsening of the bicontinuous network takes place, with channels having a characteristic diameter $a(t)$. Once $a(t) = d/2$, at time $t_{d/2}$, the wetting layers start to deplete and l_w begins to reverse its growth. Since both l_w and the coarsening process are linear with time, clearly at $t = t_{d/2}$ all films have a similar structure scaling with d. At that point, the channels rich in the

wetting phase connecting the two wetting layers have a certain density and are separated by a characteristic distance which must be proportional to d. These wetting-phase channels continue to coarsen until they are touching, at which point rupture of the nonwetting phase may occur, joining the two residual wetting layers: Since the coarsening process is itself linear with t, the time τ_{rupture} for this to happen must also increase linearly with d, precisely as observed. A quantitative comparison [20] supports this picture: Putting $a(t) = k(\gamma_{AB}/\eta)t$, we have $(d/2) = k(\gamma_{AB}/\eta)t_{d/2}$, and taking $t_{d/2} \approx 30$ s for a 1 μm thick film [as suggested by Fig. 4(a)], we find the value of the constant prefactor k to be 0.006. Bearing our approximations in mind, this compares very reasonably with the range of values $k = 0.001-0.04$ evaluated by different workers [19].

Once rupturing occurs, the bicontinuous network breaks up, with the nonwetting phase now encapsulated within the wetting phase. Droplets of the nonwetting phase attain a width W to height h ratio which minimizes their interfacial energy [6,21]. A model of the droplets as rectangloids, with $\gamma_A \gg \gamma_{AB}$, readily shows that such a minimization requires $W/h \approx \gamma_A/\gamma_{AB}$. For our fluid mixture, $\gamma_A \approx 24$ mJ/m^2, while the interfacial tension between the coexisting phases may be estimated [20], from the earlier work of Scheffold *et al.* [16], as $\gamma_{AB} \approx 0.64 \pm 0.12$ mJ/m^2, so that $\gamma_A/\gamma_{AB} \approx 38 \pm 8$. Measurements on OPIM droplet images [as in the inset of Fig. 1(d), with W taken as the droplet half-height width] show that $W/h = 18-20$ over the entire range of film thicknesses studied, which within the approximations of the model is close to the predicted value of (γ_A/γ_{AB}). Moreover, when account is taken of the known final thickness of the wetting phase in the interdroplet region together with conservation of material, a simple estimate indicates that one expects $\lambda_c/d \approx 3(W/h) = 55-60$. This fits rather closely our observation $\lambda_c = 58.5d$ [Fig. 3(a)]. The intriguing inference is that the characteristic rupture wavelength is selected by the requirement that the roughened film then minimizes its interfacial energy with respect to the encapsulated nonwetting droplets. The likely rupture mechanism itself is via coarsening of the bicontinuous network that leads (after a time τ_{rupture}) to a merging of channels bridging the two film interfaces, and their subsequent breakup within the film via Rayleigh instability.

We have shown that films of binary liquids that undergo demixing, where one component wets both confining interfaces, rupture and roughen with characteristic time and spatial scales τ_{rupture} and λ_c that increase linearly with film thickness d over more than 1.5 decades in d. This indicates at once that capillary-wave-driven liquid-liquid spinodal dewetting, previously suggested [13] for a similar system, is unlikely to be the origin of the film breakup in our system, since then one would expect $\lambda_c \propto d^2$ and $\tau_{\text{rupture}} \propto d^6$ [22]. Rather, a self-similar structure whose dimensions scale with d is indicated. The large prefactor for the $\lambda_c(d)$ variation—comparable with the ratio of interfacial tensions (γ_A/γ_{AB})—suggests the rupturing wavelength may be minimizing the surface energy of the emerging pattern, where droplets of the nonwetting phase are encapsulated by the wetting one.

We thank L. J. Fetters for kindly supplying the polymers, J. Jopp for performing the OPIM measurements, and H. Grüll, T. Kerle, and T. A. Witten for useful suggestions and discussions. The German-Israel Foundation (GIF), the Minerva Foundation, and the U.S.-Israel BSF are gratefully acknowledged for support of this work.

*Author to whom correspondence should be addressed: Physical and Theoretical Chemistry Laboratory, Oxford University, Oxford OX1 3QZ, United Kingdom.
Electronic addresses: jacob.klein@chemistry.ox.ac.uk
jacob.klein@weizmann.ac.il

[1] F. Brochard-Wyart and J. Daillant, Can. J. Phys. **68**, 1084–1088 (1990).
[2] P. G. deGennes, Rev. Mod. Phys. **57**, 827–863 (1985).
[3] L. Leger and J. F. Joanny, Rep. Prog. Phys. **55**, 431–486 (1992).
[4] A. Vrij, Discuss. Faraday Soc. **42**, 23 (1967).
[5] F. Bruder and R. Brenn, Phys. Rev. Lett. **69**, 624–627 (1992).
[6] A. Karim *et al.,* Macromolecules **31**, 857–862 (1998).
[7] P. Keblinski *et al.,* Phys. Rev. Lett. **76**, 1106–1109 (1996).
[8] G. Krausch, C. A. Dai, E. J. Kramer, and F. S. Bates, Ber. Bunsen-Ges. Phys. Chem. **98**, 446–448 (1994).
[9] W. Straub *et al.,* Europhys. Lett. **29**, 353–358 (1995).
[10] H. Tanaka, Europhys. Lett. **24**, 665–671 (1993).
[11] J. Bodensohn and W. I. Goldburg, Phys. Rev. A **46**, 5084–5088 (1992).
[12] H. Tanaka, Phys. Rev. Lett. **70**, 2770–2773 (1993).
[13] H. Wang and R. J. Composto, Europhys. Lett. **50**, 622–627 (2000).
[14] U. K. Chaturvedi *et al.,* Appl. Phys. Lett. **56**, 1228–1230 (1990).
[15] T. Kerle *et al.,* Acta Polym. **48**, 548–552 (1997).
[16] F. Scheffold *et al.,* J. Chem. Phys. **104**, 8786–8794 (1996).
[17] H. Wang and R. J. Composto, Phys. Rev. E **61**, 1659–1663 (2000).
[18] E. D. Siggia, Phys. Rev. A **20**, 595–605 (1979).
[19] H. Tanaka, Phys. Rev. E **54**, 1709–1714 (1996).
[20] The viscosity of $d95$ at 150 °C is evaluated by interpolation from the study of Carrella *et al.* [Macromolecules **17**, 2775 (1984)] as $\eta = 250 \pm 50$ Pa s. The interfacial energy $\gamma_{AB} = 0.6$ mJ/m^2 is evaluated using the Helfand formula $\gamma = k_B T a \rho_0 (\chi/6)^{1/2}$, and the appropriate parameters $a = 0.58$ nm, $\rho_0 = 1.12 \times 10^{28}$ m^{-3}, $\chi = 2.67 \times 10^{-3}$ for the two components.
[21] S. Kumar (private communication).
[22] F. Brochard-Wyatt, P. Martin, and C. Redon, Langmuir **9**, 3682–3690 (1993).